Potential impact of predation by larval Spanish mackerel on larval anchovy in the central Seto Inland Sea, Japan

Wataru Deguchi[1], Tatsunori Fujita[2], Michio Yoneda[3], Naoaki Kono[4], Masayuki Yamamoto[2], Kaito Harada[1], Jun Shoji[5], Takeshi Tomiyama[1]

[1] Graduate School of Integrated Sciences for Life, Hiroshima University, Higashi-Hiroshima 739-8528, Japan
[2] Kagawa Prefectural Fisheries Experimental Station, Takamatsu 761-0111, Japan
[3] Fisheries Technology Institute, Japan Fisheries Research and Education Agency, Imabari 794-2305, Japan
[4] Fisheries Resources Institute, Japan Fisheries Research and Education Agency, Hatsukaichi 739-0452, Japan
[5] Faculty of Marine Science and Technology, Fukui Prefectural University, Obama 917-0003, Japan

Corresponding author: T. Tomiyama (tomiyama@hiroshima-u.ac.jp)

Highlights

- Catch of larval anchovy has drastically reduced in Hiuchi-nada in the last decade.
- High mortality of anchovy larvae before recruitment is suspected.
- The top-down control by predatory Spanish mackerel larvae was examined.
- Larval abundance was high in both species in 2018.
- Estimated consumption of Spanish mackerel accounted for <4% of the total population.

Abstract

Japanese anchovy is used as an essential dried fish material from the larval to adult stages. In the central Seto Inland Sea, Japan, the catch of larval anchovy has markedly decreased to <3.9% of the maximum recorded in 2002 since 2013; however, the reason causing this reduction has not been well understood. The abundance of recruit fish, including larvae and early juveniles, has decreased in the last decade, despite abundant eggs, suggesting that the majority of larvae do not survive before recruitment. In contrast, the stock of Japanese Spanish mackerel, whose larvae are the major predator of larval anchovy, has increased in the Seto Inland Sea. It is hypothesized that an increase in the density of Spanish mackerel may have a top-down control on the decrease in anchovy recruitment by an increase in predation opportunities. In this study, we investigated the abundance of Spanish mackerel and anchovy larvae using a bongo net in the field in 2018 and 2019. The average densities of larvae in late May were 1.5–3.3 individuals (inds) / 100 m^3 and 1,058–1,346 inds / 100 m^3 for the Spanish mackerel and the anchovy, respectively; both were higher than those in 2002–2005. We constructed a Stella model, simulating the growth and survival of larval anchovy until they reached the commercial sizes by taking into account consumption by larval Spanish mackerel. The model suggested that the consumption of larval anchovy by larval Spanish mackerel accounted for <4% of the initial abundance of anchovy in 2018, which was not greater than that in 2005. In contrast, the reduction in the growth rates of larval anchovy due to reduced maternal conditions can adversely affect their survival. Thus, the results did not fully support the hypothesis mentioned above.

Keywords: top-down control; predator-prey interaction; simulation model; population dynamics

1. Introduction

Small pelagic fishes such as anchovies and sardines are in high demand for dried fish products worldwide. They also serve as "forage fish", in linking lower to higher trophic levels (Pikitch et al., 2014). Understanding their population dynamics, along with bottom-up and top-down climatic processes, is a critical challenge for sustainable fisheries and ecosystem conservation (Lynam et al., 2017).

Japanese anchovy *Engraulis japonicus* (hereinafter called anchovy) is the most important target for dried fish in Japan. In particular, larval anchovy (mostly 20–35 mm standard length [SL] and >20 days old; Zenitani et al., 2009, 2011) are in high demand and important for coastal fisheries in Japan, with annual landings of 47–75 thousand tons of larvae from 2000 to 2019 (Statistical Survey on Marine Fishery Production, Ministry of Agriculture, Forestry and Fisheries in Japan). The Seto Inland Sea, a semi-closed sea (Fig. 1) and a highly productive area, accounted for 32–56% of the total landings of larval anchovy in Japan from 2000 to 2019. In Hiuchi-nada, the central Seto Inland Sea, anchovy spawning occurs from April to August, and larvae reaching commercial sizes (recruit fish) are caught from June to September (Fujita et al., 2021). However, despite adequate egg production, the landings of larval anchovy have markedly decreased to <3.9% of the peak of 2002 in the last decade (Fig. 2). Fujita et al. (2021) suggested that the increased intraspecific competition for prey among anchovy cohorts in early life stages may be one of the factors contributing to the recruitment failure. Yoneda et al. (2022) suggested that the recent low prey availability experienced by adult anchovy reduces the survival of their offspring. Further research on the potential factors influencing larval survival is necessary to understand the implementation of effective fishery management.

Predation is a key factor that affects early-stage survival (Baily and Houde, 1989; Leggett and Deblois, 1994). In the Seto Inland Sea, Japanese Spanish mackerel *Scomberomorus niphonius* (hereinafter called Spanish mackerel) exhibits strong piscivory from the first feeding stage, that is, 5–6 days after hatching (Kono et al., 2014), and anchovy is the most dominant prey item in their stomachs (Shoji et al., 1997). The stock of Spanish mackerel in the Seto Inland Sea has increased, and the catch in 2020 is 14 times greater than in 1998 (Fig. 2). The central Seto Inland Sea is one of the main spawning grounds of Spanish mackerel (Shoji and Tanaka, 2005a; Katamachi et al., 2022), in which the spawning season occurs from May to June (Kishida and Aida, 1989). Spanish mackerel larvae are the most abundant from late May to early June, overlapping the main fishing season of anchovy larvae

(Shoji et al., 1999a). Thus, it is assumed that the inconsistency between increasing anchovy egg abundance and decreasing anchovy recruitment may be partly due to increased predation opportunities by Spanish mackerel larvae; however, the amount of predation through prey-predator relationships between these two species is yet to be estimated.

This study aimed (1) to evaluate the potential impact of predation by Spanish mackerel larvae on the recruitment of larval anchovy in Hiuchi-nada through field surveys and model simulation, and (2) to test the hypothesis that an increase in the density of Spanish mackerel may have a top-down control on decrease in anchovy recruitment due to an increase in predation opportunities. In the field surveys conducted in 2018 and 2019, we investigated the larval abundance of the two species to test whether their densities increased from the past; the densities were also investigated in 2002–2005. Furthermore, we also constructed a model to simulate the growth and survival of larval anchovy concerning predation by Spanish mackerel larvae. Using this model, we assessed predation mortality in larval anchovy by larval Spanish mackerel in 2005 and 2018. In addition, we examined the response of anchovy survival to the 10-fold density of Spanish mackerel larvae in 2018 to test whether the increased number of Spanish mackerel larvae could explain the recruitment failure of anchovy. Additionally, we simulated the survival of anchovy larvae with reduced growth rates associated with the reduced maternal conditions (Yoneda et al., 2022) to evaluate the impacts of both top-down and bottom-up effects.

2. Materials and methods

2.1. Field survey

The survey was conducted in Hiuchi-nada, the central Seto Inland Sea (Fig. 1). Spanish mackerel spawns around central Hiuchi-nada, and larvae are transported to the southern area along with the southward ocean current (Shoji and Tanaka, 2005a). Therefore, sampling stations were set up in the southern and eastern areas (Fig. 1). Larvae were collected using a bongo net with a mouth diameter of 60 cm and mesh size of 0.335 mm (Fig. S1) in May and June 2018–2019. Spanish mackerel larvae are abundant in the middle or bottom layers during the day, while they also appear in the surface layer at night due to their diel vertical migration (Shoji et al., 1999b). The bongo net was towed obliquely to cover the larval distribution layers. Flow meters were attached to the net mouth to measure the volume of filtered water.

The survey in the southern area was conducted during daytime and nighttime at three stations in May 2018, May 2019, and June 2019. The bongo net was towed by the training and research vessel Toyoshiomaru (256 tons) of Hiroshima University at a speed of 2 knots for 10 min (two round trips). The volume of water filtered by the net was 206 ± 56 m^3 (mean ± SD, n = 14) in May 2018, 244 ± 45 m^3 (n = 12) in May 2019, and 166 ± 17 m^3 in June 2019 (n = 12). The survey in the eastern area was conducted during the daytime at seven stations from May to June in 2018 and 2019. The bongo net was towed by the research vessel Yakuri (19 tons) of the Kagawa Prefectural Fisheries Experimental Station for 4 min (one round trip). The volume of water filtered by the net was 32 ± 6 m^3 (n = 35).

The collected specimens were immediately preserved onboard in 5% seawater formalin (southern area) or were kept in ice and brought to the laboratory (eastern area).

2.2. Measurements and analyses

The larvae of the Spanish mackerel and anchovy were sorted and counted from the bongo net specimens. To reveal the species composition and proportion of Spanish mackerel or anchovy in the collected larvae, other fish larvae were identified to species or lowest possible levels only for the specimens in May 2018. The SL of the larvae was measured to the nearest 0.1 mm, using a digital caliper under a stereomicroscope. The density was calculated by dividing the number of individuals collected from the volume of filtered water (individuals per 100 m^3). The net efficiency was not taken into consideration.

2.3. Simulation model

A model based on the literature and our data was constructed to simulate the growth and survival of both anchovy and Spanish mackerel larvae. The consumption of larval anchovy by predators was calculated based on the dry weight (mg).

2.3.1. Survival and growth of larval anchovy

The daily survival rate of larval anchovy depends on the density of copepod nauplii which is <100 µm, and the survival rate is constant at 0.89 under nauplius densities of >5 individuals/L (Zenitani et al., 2007). The daily survival rate was set to 0.89 to simplify the model because the densities of the copepod nauplius were high in recent years (Fujita et al., 2021).

The SL at hatching in response to water temperature has not been elucidated, but the SL at the first feeding (SL_F) incorporating the effect of water temperature (WT, °C) was shown (Fujita et al., 2021): $SL_F = \exp(-0.019 \times WT + 1.74)$. It takes approximately five days from hatching to the first feeding at 16 °C in anchovy (Fujita et al., 2021). According to Fukuhara (1983), larval anchovy grows by 1 mm after four days of hatching. Thus, the SL at hatch (SL_H) was set as follows: $SL_H = \exp(-0.019 \times WT + 1.74) - 1.25$. The daily growth rate of anchovy larvae (GR, mm/d), estimated by otolith microstructure analyses, showed a strong correlation with WT in Osaka Bay, eastern Seto Inland Sea (Tsujino and Watari, 2001): $GR = 0.6972 \times \ln(WT) - 1.3101$. To calculate the SL on each date, the growth rate of larvae was considered to be 0.25 mm/d until five days after hatching, and thereafter, the above-mentioned formula was used. The body dry weight (BDW, mg) of anchovy larvae was calculated using the formula (Shoji and Tanaka, 2005b): $BDW = 2.045 \times 10^{-4} \times SL^{3.385}$.

2.3.2. Survival and growth of larval Spanish mackerel

In the field survey, the daily mortality (M) of Spanish mackerel larvae was estimated to be 0.625–0.784 (Shoji et al., 2005). In this study, the daily survival rate (e^{-M}) with M = 0.7 was used in the model. A laboratory experiment revealed that Spanish mackerel hatch with a total length of 4.6 mm, absorb egg yolk after five days of hatching, and start feeding after six days of hatching (Kono et al., 2014) with a total length of 5.6 mm (Shoji and Tanaka, 2001). Although many larvae of SL <5 mm were collected in our field surveys (see results), the SL at the first feeding was set to be 5.3 mm, assuming a total length of 5.6 mm. We incorporated larvae after the onset of feeding into the model.

The growth rate of wild Spanish mackerel is approximately 1 mm/d until 20 days after hatching (Shoji et al., 1999a), and wild juveniles reach over 70 mm in total length (60 mm SL) 35 days after mouth opening (Fukunaga et al., 1982). Based on these data, the growth rate was assumed to be 1 mm/d until 15 days after the first feeding and thereafter set to 2 mm/d. Because the daily food consumption (ration) on a dry weight basis was 66.1% at 18.6 °C and 82.6% at 21.2 °C (Shoji and Tanaka, 2005b), it was set to 70% below 19 °C and 80% above 19 °C. To estimate the BDW of Spanish mackerel larvae, the following formula was used (Shoji et al., 2001): $BDW = 2.115 \times 10^{-4} \times SL^{3.587}$.

The SL of anchovy larvae vulnerable to predation is assumed to be in the range of 50–100% of the SL of Spanish mackerel larvae, following stomach content analysis of wild larvae and juveniles (Shoji and Tanaka, 2005b). The number of anchovy larvae consumed daily was estimated by dividing the daily food consumption of the Spanish mackerel larvae with the BDW of the anchovy larvae. It was assumed that Spanish mackerel larvae only feed on anchovy larvae and that they show a size preference for larger prey among the available sizes. These assumptions were set to simplify the model and were based on previous studies; wild Spanish mackerel larvae mostly consumed fish larvae (Shoji et al., 1997; Shoji and Tanaka, 2001), and a strong positive relationship was observed between prey size and the body size of Spanish mackerel larvae (Shoji et al., 1997; Shoji and Tanaka, 2005b).

2.3.3. Dataset and model simulation

Using the 2018 dataset, we constructed a model that expresses the dynamics of larval density and growth of Spanish mackerel and anchovy larvae (Fig. 3, Fig. S2, Appendix S1). To simplify the model, a simulation was performed based on density and SL data without distinguishing the southern and eastern areas. We set four cohorts of anchovy larvae that hatched on May 1 (cohort A1), May 11 (cohort A2), May 21 (cohort A3), and May 31 (cohort A4), while we set three cohorts of Spanish mackerel larvae that started feeding on May 11 (cohort M1), May 21 (cohort M2), and May 31 (cohort M3). A cohort of Spanish mackerel that started feeding on May 1 was not considered because no Spanish mackerel larvae were caught during sampling in late April in 2002–2005 (Zenitani and Kono, unpubl. data).

Water temperature was incorporated as a physical environmental factor. We used monthly water temperature data at a depth of 10 m observed at four stations in the eastern area, monitored by the Kagawa Prefectural Fisheries Experimental Station. The data for each day was collected based on the linear relationship between the date and the water temperature from April to July ($r^2 > 0.96$; Fig. S3).

The simulation was performed using Stella Professional version 1.0.3 (isee systems incorporated). Stella is a useful tool for modelling dynamic systems (Costanza et al., 1998). The model was run for 60 days from May 1 to June 29 and the growth and survival of anchovy during the period from hatching to recruitment (reaching commercial sizes of 20 mm SL) were evaluated for each anchovy cohort. The survival rate and cumulative consumption of Spanish mackerel larvae were calculated. To examine the variability in predation mortality, it was assumed that natural mortality, such as harvest through fisheries or predation by other predators, was independent of predation by Spanish mackerel larvae.

The model was run under three scenarios: Scenario 1 assumed the situation of 2018, Scenario 2 assumed the increased density of Spanish mackerel with other factors unchanged from Scenario 1. Scenario 3 assumed the reduced growth rates of anchovy (0.76 fold of Scenario 1) by taking the result of Yoneda et al. (2022) into consideration: growth rates of larvae from females under low food availability were ~76% of those of larvae from females under high food availability. For Scenarios 1–3, the initial density of larval anchovy was considered 300 inds / 100 m^3 for anchovy cohorts A1 and A2, and 3,000 inds / 100 m^3 for anchovy cohorts A3 and A4, according to the survey data from 2018 (see results). Similarly, the initial density was set as 1, 6, and 11 inds / 100 m^3 for cohorts M1, M2, and M3, respectively, assuming the situation in 2018 for Scenarios 1 and 3. For Scenario 2, the initial density of Spanish mackerel was 10-fold that of Scenario 1 to examine the response of anchovy survival to the rapid increase in Spanish mackerel.

To examine whether the predation mortality of anchovy by Spanish mackerel increased in the last decade, we also ran the model with different densities of cohorts considering the survey data in 2005. A similar survey using a bongo net was conducted in Hiuchi-nada from May to June 2002–2005 (Zenitani et al., 2011; Zenitani and Kono, unpubl. data), during which the density of Spanish mackerel larvae was the highest in 2005 (Figs. S4, S5). Initial densities were given as 300 inds / 100 m^3 for cohorts A1–A3, 1,000 inds / 100 m^3 for A4, and 1, 2, and 5 inds / 100 m^3 for cohorts M1, M2, and M3, respectively. Similarly, water temperature was given using the data from 2005.

2.3.4. Sensitivity analysis

The model assumed that the survival rates of Spanish mackerel and anchovy are constant, and the daily low survival rate of approximately 0.5 (M = 0.7) for Spanish mackerel limits the predation of anchovy. However, it is expected that the survival rate of Spanish mackerel will increase with an increase in body size or with higher prey availability. Therefore, in Scenario 1, we examined the variability in the proportion of predation by Spanish mackerel in response to the survival rate of Spanish mackerel using sensitivity analysis. The survival rate changed from 0.2 to 0.8 with an interval of 0.2, corresponding to the M from 1.6 to 0.2.

3. Results

3.1. Occurrence of Spanish mackerel and anchovy larvae

Spanish mackerel larvae were observed from early May to mid-June 2018 (Fig. 4). The larval densities of both Spanish mackerel and anchovy exhibited single peaks in early June. The density of anchovy larvae was higher in 2018 than in 2019 and relatively high in the eastern area. The densities were higher in early June than in late May 2018 for both Spanish mackerel and anchovy larvae (Figs. S4).

The anchovy was the most dominant species (64.7%) among the larvae collected in the southern area in May 2018 (Table 1). Spanish mackerel accounted for 1.3% of the total larval sample. In May and June 2019, 71 and 5 individuals of Spanish mackerel larvae (2.3–5.8 mm SL in May and 2.4–5.0 mm in June) and 27,259 and 620 individuals of anchovy larvae (1.7–8.9 mm SL in May and 1.4–9.3 mm in June) were collected, respectively. Larval Spanish mackerel were mostly mouth-opened in 2018, whereas a large number of larvae collected in 2019 were unopened (Fig. 5). In the eastern area, 27 individuals of Spanish mackerel larvae were collected in 2018, whereas no individuals were found in 2019.

3.2. Model simulation

The model based on Scenario 1 well reflected the densities of Spanish mackerel and anchovy larvae (Fig. S6). The duration from hatching to recruitment (reaching 20 mm SL) was estimated to be 31, 29, 28, and 27 days for cohorts A1, A2, A3, and A4, respectively. Following SL of the larvae, anchovy cohort A1 was targeted by Spanish mackerel cohorts M1, A2 by M1 and M2, A3 by M2 and M3, and A4 by M3. The survival rate of anchovy cohorts was estimated to be 3.8% in total (Table 2). In addition, the proportion of predation mortality by Spanish mackerel relative to the initial population size was estimated to be 2.7% in total.

In Scenario 2, which assumed an increase in predation pressure by Spanish mackerel, the survival rate of anchovy decreased to 2.7% in total. Predation by Spanish mackerel increased to 27.4%. In Scenario 3, due to the reduced growth rates of larval anchovy, the duration from hatching to recruitment was estimated to be 38, 36, 34, and 33 days for cohorts A1, A2, A3, and A4, respectively. The survival rate of anchovy was lower than that in Scenario 2 although predation by Spanish mackerel slightly increased from Scenario 1 (Table 2).

In the model assuming the situation in 2005 (Fig. S7), the survival rate of anchovy cohort was similar to that of Scenario 1, whereas the proportions of Spanish mackerel predation was greater than that of Scenario 1.

The sensitivity analysis showed that the variation in anchovy survival rate in response to Spanish mackerel survival rate in Scenario 1 was relatively less (Table 3). The increase in the survival rate of the anchovy cohort was 0.0–1.7% when the survival rate of the Spanish mackerel was 0.2 compared to the case of 0.8. Predation by Spanish mackerel increased with their higher survival rate, but the proportion of predation mortality for anchovy cohorts at the daily survival rate of 0.6 was not largely different from that at 0.4, except for cohort A1 (Table 3).

4. Discussion

This study clarified that the recent decline in the survival rate of larval anchovy from hatching to recruitment was rarely attributable to the increased abundance of larval Spanish mackerel. Our predator-prey model, incorporating daily consumption, growth, and mortality in both Spanish mackerel and anchovy larvae, revealed that the consumption of larval anchovy by the larval Spanish mackerel accounted for <4% of the initial abundance in 2018 (Table 2), suggesting a small proportion of the Spanish mackerel predation on the mortality of anchovy larvae. The model simulating 2005 showed that the relative predation intensity of Spanish mackerel was higher in 2005 than in 2018. Furthermore, the survival of anchovy before recruitment did not decrease largely, even under the 10-fold density of Spanish mackerel using the 2018 dataset (Scenario 2) although the proportion of larval anchovy consumed by larval Spanish mackerel greatly increased. This scenario is unrealistic without prey increase for the larval Spanish mackerel as well, because larval Spanish mackerel are easily susceptible to starvation mortality under low prey concentration (Shoji et al., 2002). In contrast, the survival of larval anchovy was more drastically decreased in Scenario 3, in which reduced maternal conditions led to reduced growth rates of larval anchovy. This result indicates a greater bottom-up impact on anchovy recruitment in recent years (Yoneda et al., 2022) than the increase in Spanish mackerel. Top-down control is an important issue for understanding the population dynamics of pelagic fishes (Glaser, 2011), but predation has rarely been confirmed as the major reason for the rapid decline in the forage fish population. For example, Atlantic bluefin tuna juveniles increased, but their consumption of pelagic fishes accounted for only 2% of the abundance (Van Beveren et al., 2017). Thus, the mechanisms underlying the recent decline in the catch of larval anchovy could be largely attributed to bottom-up processes rather than top-down processes. It should be noted that the degree of bottom-up process changes has not been assessed in the field and therefore the impact of bottom-up effects is one of the future issues.

During the survey of 2018–2019, both the larval density and young-of-the-year (YOY) fish abundance of Spanish mackerel were higher than those during the previous survey of 2002–2005 (Figs. S4, S5), when the Spanish mackerel stock level was low. In the Seto Inland Sea, the number of recruited wild YOY Spanish mackerel estimated from landings in fish markets was also greater in 2018 and 2019 (3,080 and 2,199 thousand individuals, respectively) than in 2002–2005 (518–1,208 thousand individuals; Katamachi et al., 2022). Notably, the abundance of larval anchovy before recruitment was greater in recent years than in 2002–2005 (Fujita et al., 2021; the present study). Thus, the duration from hatching at approximately 3 mm to recruitment at 20 mm should be the critical period for the survival of larval anchovy, and the survival during this period is considered to decrease drastically in recent years: recruit abundance relative to the abundance of eggs or that of pre-recruit larvae has markedly decreased in the last decade (Fujita et al., 2021). The ratio of larval anchovy to larval Spanish mackerel in late May was 1190, 280, 1356, 208, 408, and 684 in 2002, 2003, 2004, 2005, 2018, and 2019, respectively, indicating that susceptibility to predation did not increase during 2018–2019 compared to that during 2002–2005.

The seasonal changes in the densities of Spanish mackerel and anchovy larvae coincided well in 2018 (Fig. 4). The density of larval anchovy was >400-fold higher than that of Spanish mackerel larvae in both late May and early June 2018, suggesting high prey availability for Spanish mackerel. Moreover, the spatial distribution of larvae also coincided between the two species (Figs. S8, S9). These characteristics are advantageous for the survival of Spanish mackerel because of the low starvation tolerance of Spanish mackerel larvae shortly after the first feeding (Shoji et al., 2002). In our model, the daily survival rate of Spanish mackerel was set at a constant of $M = 0.7$, but M should decrease as Spanish mackerel grows. The starvation tolerance of juvenile Spanish mackerel is higher than larvae (Harada et al., 2021), hence it may be appropriate to set the survival rate of juveniles ≥12 mm (Kishida, 1991) to be higher than that of larvae in the model. Notably, the spatial overlap between larval anchovy and larval Spanish mackerel was reduced in 2019. This result was due to the absence of Spanish mackerel larvae from specimens collected in the eastern areas. The small volume of water filtered might have affected the absence of Spanish mackerel larvae.

In our model, the survival of anchovy larvae was similar in 2005 and 2018 (Scenario 1), which is inconsistent with the fact that the catch of larval anchovy extremely differed between the two years (Fig. 2). Thus, the incorporation of other processes is important. For example, information on other predators was not considered in our model. Considering anchovy the most important prey for several piscivorous fishes (Tomiyama and Kurita, 2011; Niino et al., 2017), it would be advantageous to include predation pressures by other predators in the model to strengthen the validity of the natural mortality of anchovy larvae. Actually, juvenile Japanese flounder *Paralichthys olivaceus* feed on larval anchovy in Hiuchi-nada in June (Yamada et al., 2020). Invertebrates such as jellyfish are also predators or competitors for fish larvae (Cowan et al., 1996; Zenitani et al., 2017). Furthermore, this study did not incorporate changes in prey availability for larval anchovy, although the copepod nauplius density was higher in 2015–2019 than in 2002–2005 (Fujita et al., 2021). Future models may add more variables, such as the effects of temperature and prey availability on anchovy reproduction, because higher temperature and prey abundance would result in shorter spawning intervals (Zenitani et al., 2005; Yoneda et al., 2014) as well as smaller anchovy egg sizes (Yoneda et al., 2022).

This study considered the potential impacts of Spanish mackerel larvae predation on anchovy larvae survival. Because the bottom-up impacts appeared to be greater (Yoneda et al., 2022, this study), the recent decline in the recruitment of larval anchovy can largely be attributed to low prey availability for adult anchovy. Furthermore, dried fish production in Japan is supported by the biological production of anchovy, and the stock level has declined for populations other than the Seto Inland Sea population. To ensure a sustainable dried fish industry, the population dynamics of anchovy should be monitored.

Acknowledgements: We thank Nakaguchi, K., Yamaguchi, S., other staff of Training and research vessel Toyoshiomaru, and staff of Kagawa Prefectural Fisheries Experimental Station for their help in the larval collection in the field. We also thank the two anonymous reviewers for their helpful comments on the manuscript. This work was partly supported by the Fisheries Agency of Japan and Japan Fisheries Research and Education Agency and by JSPS KAKENHI Grant Number 19K06207.

Reference

Baily, K.M., Houde, E.D., 1989. Predation on eggs and larvae of marine fishes and the recruitment problem. Adv. Mar. Biol. 25, 1–83. https://doi.org/10.1016/S0065-2881(08)60187-X

Costanza, R., Duplisea, D., Kautsky, U., 1998. Ecological modelling on modelling ecological and economic systems with STELLA. Ecol. Modell. 110, 1–4. https://doi.org/10.1016/S0304-3800(98)00099-4

Cowan, J.H., Jr, Houde, E.D., Rose, K.A., 1996. Size-dependent vulnerability of marine fish larvae to predation: an individual-based numerical experiment. ICES J. Mar. Sci. 53, 23–37. https://doi.org/10.1006/jmsc.1996.0003

Fujita, T., Yamamoto, M., Kono, N., Tomiyama, T., Sugimatsu, K., Yoneda, M., 2021. Temporal variations in hatch date and early survival of Japanese anchovy (*Engraulis* *japonicus*) in response to environmental factors in the central Seto Inland Sea, Japan. Fish. Oceanogr. 30, 527–541. https://doi.org/10.1111/fog.12535

Fukuhara, O., 1983. Development and growth of laboratory reared *Engraulis japonica* (Houttuyn) larvae. J. Fish Biol. 23, 641–652. https://doi.org/10.1111/j.1095-8649.1983.tb02943.x

Fukunaga, T., Ishibashi, N., Mitsuhashi, N., 1982. Artificial fertilization and seedling propagation of Spanish mackerel. Saibai Giken 11, 29–48. (in Japanese)

Glaser, S.M., 2011. Do albacore exert top-down pressure on northern anchovy? Estimating anchovy mortality as a result of predation by juvenile north pacific albacore in the California current system. Fish. Oceanogr. 20, 242–257. https://doi.org/10.1111/j.1365-2419.2011.00582.x

Harada, K., Morita, T., Deguchi, W., Yamamoto, M., Fujita, T., Tomiyama, T., 2021. High-temperature and starvation tolerances of juvenile Japanese Spanish mackerel *Scomberomorus niphonius*. Fish. Sci. 87, 513–519. https://doi.org/10.1007/s12562-021-01521-w

Katamachi, D., Yasuda, T., Kono, N., Takahashi, M., 2022. Stock assessment and evaluation for the Seto Inland Sea stock of Japanese Spanish mackerel (fiscal year 2021). Marine fisheries stock assessment and evaluation for Japanese waters (fiscal year 2021/2022). Fisheries Agency and Fisheries Research and Education Agency of Japan, FRA-SA2021-RC03-2. (in Japanese)

Kishida, T., 1991. Fluctuations in year-class strength of Japanese Spanish mackerel in the central Seto Inland Sea. Nippon Suisan Gakkaishi 57, 1103–1109. https://doi.org/10.2331/suisan.57.1103

Kishida, T., Aida, K., 1989. Maturation and spawning of Japanese Spanish mackerel in the central and western waters of the Seto Inland Sea. Nippon Suisan Gakkaishi 55, 2065–2074. (in Japanese with English abstract) https://doi.org/10.2331/suisan.55.2065

Kono, N., Takahashi, M., Shima, Y., 2014. Time of formation of incremental and discontinuous zones on sagittal otoliths of larval Japanese Spanish mackerel *Scomberomorus niphonius*. Nippon Suisan Gakkaishi 80, 21-26. (in Japanese with English abstract) https://doi.org/10.2331/suisan.80.21

Leggett, W.C., Deblois, E., 1994. Recruitment in marine fishes: Is it regulated by starvation and predation in the egg and larval stages? Neth. J. Sea Res. 32, 119–134. https://doi.org/10.1016/0077-7579(94)90036-1.

Lynam, C.P., Llope, M., Möllmann, C., Helaouët, P., Bayliss-Brown, G.A., Stenseth, N.C., 2017. Interaction between top-down and bottom-up control in marine food webs. Proc. Nat. Acad. Sci. 114, 1952–1957. https://doi.org/10.1073/pnas.1621037114

Niino, Y., Shibata, J., Tomiyama, T., Sakai, Y., Hashimoto, H., 2017. Feeding habits of the cutlassfish *Trichiurus japonicus* around Hiuchi-Nada, central Seto Inland Sea, Japan. Nippon Suisan Gakkaishi 83, 34–40. https://doi.org/10.2331/suisan.16-00032

Pikitch, E.K., et al. 2014. The global contribution of forage fish to marine fisheries and ecosystems. Fish Fish. 15, 43–64. https://doi.org/10.1111/faf.12004

Shoji, J., Tanaka, M., 2001. Strong piscivory of Japanese Spanish mackerel larvae from their first feeding. J. Fish Biol. 59, 1682–1685. https://doi.org/10.1111/j.1095-8649.2001.tb00232.x

Shoji, J., Tanaka, M., 2005a. Distribution, feeding condition, and growth of Japanese Spanish mackerel (*Scomberomorus niphonius*) larvae in the Seto Inland Sea. Fish. Bull. 103, 371–379.

Shoji, J., Tanaka, M., 2005b. Daily ration and prey size of juvenile piscivore Japanese Spanish mackerel. J. Fish Biol. 67, 1107–1118. https://doi.org/10.1111/j.0022-1112.2005.00813.x

Shoji, J., Kishida, T., Tanaka, M., 1997. Piscivorous habits of Spanish mackerel larvae in the

Seto Inland Sea. Fish. Sci. 63, 388–392. https://doi.org/10.2331/fishsci.63.388

Shoji, J., Maehara, T., Tanaka, M., 1999a. Short-term occurrence and rapid growth of Spanish mackerel larvae in the central waters of the Seto Inland Sea, Japan. Fish. Sci. 65, 68–72. https://doi.org/10.2331/fishsci.65.68

Shoji, J., Maehara, T., Tanaka, M., 1999b. Diel vertical movement and feeding rhythm of Japanese Spanish mackerel larvae in the central Seto Inland Sea. Fish. Sci. 65, 726–730. https://doi.org/10.2331/fishsci.65.726

Shoji, J., Maehara, T., Aoyama, M., Fujimoto, H., Iwamoto, A., Tanaka, M., 2001. Daily ration of Japanese Spanish mackerel *Scomberomorus niphonius* larvae. Fish. Sci. 67, 238–245. https://doi.org/10.1046/j.1444-2906.2001.00246.x

Shoji, J., Aoyama, M., Fujimoto, H., Iwamoto, A., Tanaka, M., 2002. Susceptibility to starvation by piscivorous Japanese Spanish mackerel *Scomberomorus niphonius* (Scombridae) larvae at first feeding. Fish. Sci. 68, 59–64. https://doi.org/10.1046/j.1444-2906.2002.00389.x

Shoji, J., Maehara, T., Tanaka, M., 2005. Larval growth and mortality of Japanese Spanish mackerel (*Scomberomorus niphonius*) in the central Seto Inland Sea, Japan. J. Mar. Biol. Assoc. U.K. 85, 1255–1261. https://doi.org/10.1017/S0025315405012403

Tomiyama, T., Kurita, Y., 2011. Seasonal and spatial variations in prey utilization and condition of a piscivorous flatfish *Paralichthys olivaceus*. Aquat. Biol. 11, 279–288. https://doi.org/10.3354/ab00319

Tsujino, K., Watari, T., 2001. Daily growth of Japanese anchovy larvae *Engraulis japonica* in Osaka Bay. Bull. Osaka Prefect. Fish. Exp. Stn 13, 11–18 (in Japanese)

Van Beveren, E., Fromentin, J.M., Bonhommeau, S., Nieblas, A.E., Metral, L., Brisset, B., Jusup, M., Bauer, R.K., Brosset, P., Saraux, C., 2017. Predator–prey interactions in the face of management regulations: changes in Mediterranean small pelagic species are not due to increased tuna predation. Can. J. Fish. Aquat. Sci. 74, 1422–1430. https://doi.org/10.1139/cjfas-2016-0152

Yamada, T., Maehara, T., Watanabe, A, Takashima, K., Tomiyama, T., 2020. Annual variation in the prey utilization of juvenile Japanese flounder in southwestern Hiuchi-Nada, Seto Inland Sea, Japan. Region. Stud. Mar. Sci. 39, 101453. https://doi.org/10.1016/j.rsma.2020.101453

Yoneda, M., Kitano, H., Tanaka, H., Kawamura, K., Selvaraj, S., Ohshimo, S., Matsuyama, M., Shimizu, A., 2014. Temperature- and income resource availability-mediated variation in reproductive investment in a multiple-batch-spawning Japanese anchovy. Mar. Ecol. Prog. Ser. 516, 251–262. https://doi.org/10.3354/meps10969

Yoneda, M., Fujita, T., Yamamoto, M., Tadokoro, K., Okazaki, Y., Nakamura, M., Takahashi, M., Kono, N., Matsubara, T., Abo, K., Xinyu, G., Yoshie, N., 2022. Bottom-up processes drive reproductive success of Japanese anchovy in an oligotrophic sea: A case study in the central Seto Inland Sea, Japan. Prog. Oceanogr. 206, 102860. https://doi.org/10.1016/j.pocean.2022.102860

Zenitani, H., Kono, N., Tsukamoto, Y., 2005. Effect of sea water temperature and condition factor on variability of spawning interval and relative batch fecundity of Japanese anchovy in the Seto Inland Sea in summer and autumn. Nippon Suisan Gakkaishi 71, 821–823. (in Japanese)

Zenitani, H., Kono, N., Tsukamoto, Y., 2007. Relationship between daily survival rates of larval Japanese anchovy (*Engraulis japonicus*) and concentrations of copepod nauplii in the Seto Inland Sea, Japan. Fish. Oceanogr. 16, 473–478. https://doi.org/10.1111/j.1365-2419.2007.00434.x

Zenitani, H., Kono, N., Tsukamoto, Y., Masuda, R., 2009. Effects of temperature, food availability, and body size on daily growth rate of Japanese anchovy *Engraulis japonicus*

larvae in Hiuchi-nada. Fish. Sci. 75, 1177–1188. https://doi.org/10.1007/s12562-009-0147-4
Zenitani, H., Kono, N., Tsukamoto, Y., 2011. Simulation of copepod biomass by a prey–predator model in Hiuchi-nada, central part of the Seto Inland Sea: does copepod biomass affect the recruitment to the shirasu (Japanese larval anchovy *Engraulis japonicus*) fishery? Fish. Sci. 77, 455–466. https://doi.org/10.1007/s12562-011-0343-x
Zenitani, H., Kono, N., Watari, S., 2017. Impact of the jellyfish *Aurelia aurita* on the anchovy fishery stock in Hiuchi-nada, central Seto Inland Sea, Japan. Bull. Jpn. Soc. Fish. Oceanogr. 81, 1–17. (in Japanese with English abstract)

Table 1.

Species composition of fish larvae collected by the bongo net in the southern area in 2018

Order	Species	English name	N	Standard length (mm)
Clupeiformes	*Konosirus punctatus*	Gizzard shad	390	1.5–11.0
	Engraulis japonicus	Japanese anchovy	8,595	1.2–13.5
Aulopiformes	Synodontidae spp.	Lizardfish	122	1.9–3.5
Mugiliformes	Mugilidae spp.	Mullet	50	2.1–9.1
Gasterosteiformes	*Syngnathus schlegeli*	Seaweed pipefish	3	11.2–11.8
Beloniformes	Unidentified		6	6.2–14.9
Perciformes	*Sebastiscus marmoratus*	Marbled rockfish	5	3.1–4.2
	Scorpaenoidei sp.		1	2.5
	Pagrus major	Red seabream	2	3.2–6.8
	Acanthopagrus schlegelii	Black seabream	210	1.9–10.9
	Sparidae spp.	Seabream	45	1.5–3.8
	Sillago japonica	Japanese whiting	1	2.0
	Pomacentridae spp.	Damselfish	330	1.6–4.8
	Labridae sp.	Wrasse	1	1.4
	Gracilopterygion bapturum	Princess blenny	1	7.1
	Parablennius yatabei	Yatabe blenny	17	3.5–12.5
	Blenniidae spp.	Blenny	8	2.4–4.5
	Callionymidae spp.	Dragonet	308	1.0–8.4
	Gobiidae spp.	Goby	2,867	1.5–24.3
	Scomber spp.	Mackerel	19	2.7–6.5
	Scomberomorus niphonius	Japanese Spanish mackerel	172	1.6–11.7
Pleuronectiformes	*Pseudorhombus* spp.	Flounder	7	2.4–7.2
	Soleidae spp.	Sole	29	1.6–2.9
Tetraodontiformes	Monacanthidae spp.	Filefish	4	1.6–2.3
	Tetraodontidae	Puffer	6	1.5–2.0
Unidentified	Unidentified		87	1.0–1.8
Total			13,287	

Table 2

Results of the model simulation of anchovy cohorts survival and predation

Cohort	2018			2005
	Scenario 1	Scenario 2	Scenario 3	
Survival (%)				
A1	2.7	2.6	1.2	2.7
A2	3.2	1.6	1.4	3.2
A3	3.7	2.7	1.8	3.4
A4	4.2	2.8	2.1	4.6
Total	3.8	2.7	1.9	3.9
Predation by Spanish mackerel (%)				
A1	0.0	0.3	0.1	0.0
A2	4.0	39.6	4.6	3.9
A3	2.6	25.7	2.7	8.6
A4	3.1	30.6	3.1	4.2
Total	2.7	27.4	2.8	4.2

Scenario 1 assumed a situation in 2018. Scenario 2 assumed a 10-fold density of Spanish mackerel compared to Scenario 1. Scenario 3 assumed a 0.76-fold growth rate of anchovy in Scenario 1. The model was run for 60 days. The initial densities of larval anchovy were set as 300 inds / 100 m^3 for anchovy cohorts A1 and A2, and 3,000 inds / 100 m^3 for anchovy cohorts A3 and A4 in the models of 2018, whereas they were set as 300 inds / 100 m^3 for cohorts A1–A3 and 1,000 inds / 100 m^3 for A4 in the model of 2005. The initial densities of larval Spanish mackerel for cohorts M1, M2, and M3 were set as 1, 6, and 11 inds / 100 m^3 in Scenarios 1 and 3, 10, 60, and 110 inds / 100 m^3 in Scenario 2, and 1, 2, and 5 inds / 100 m^3 in the model of 2005.

Table 3

Sensitivity analysis of the daily survival of larval Spanish mackerel for the survival or predation by Japanese Spanish mackerel in each cohort of larval Japanese anchovy in the simulation model (Scenario 1)

Daily survival	Survival (%)				Predation by Spanish mackerel (%)			
	A1	A2	A3	A4	A1	A2	A3	A4
0.8	2.3	1.6	3.4	4.2	0.994	8.8	3.7	3.1
0.6	2.7	3.1	3.7	4.2	0.09	4.5	2.8	3.1
0.4	2.7	3.3	3.7	4.2	0.01	3.6	2.4	3.1
0.2	2.7	3.3	3.7	4.2	0.00	2.9	1.9	3.1
CV	0.06	0.30	0.04	0.00	1.76	0.53	0.28	0.00

Figure captions

Fig. 1. Map showing the study area of Hiuchi-nada, the central Seto Inland Sea. Larval collections were conducted in the shaded areas.

Fig. 2. The ratio of annual catch to the maximum catch during 1990–2020 for Japanese Spanish mackerel (JSM) in the Seto Inland Sea and for juvenile–adult Japanese anchovy (Anchovy) and larval Japanese anchovy (Larvae) in eastern Hiuchi-nada. The maximum catches were 2,946 tons in 1990 for JSM, 11,080 tons in 1991 for Anchovy, and 1,454 tons in 2002 for Larvae. Catch of JSM has increased from 1998 to 2020 whereas that of larval anchovy has decreased to <56 tons (<3.9% of the maximum) since 2013.

Fig. 3. Diagrammatic model for the consumption of anchovy larvae by Spanish mackerel larvae, simulated in Stella. Each cohort model involves individual growth and cohort dynamics. Only one cohort was shown for each fish species, as an example. Symbols such as the state variable (square), flow regulator (circle with a faucet), and variable (circle) are explained in Costanza et al. (1998).

Fig. 4. Seasonal changes in the larval abundances of Japanese Spanish mackerel and Japanese anchovy in 2018 and 2019. Vertical bars indicate standard deviations.

Fig. 5. Length-frequency distributions of larval Japanese Spanish mackerel (JSM) and larval Japanese anchovy collected in 2018 and 2019. The mouth opening of larval JSM was examined only for the southern area. Specimens of larval JSM were collected mostly in May, and the data were pooled for the two months survey (May and June).

Fig. 1

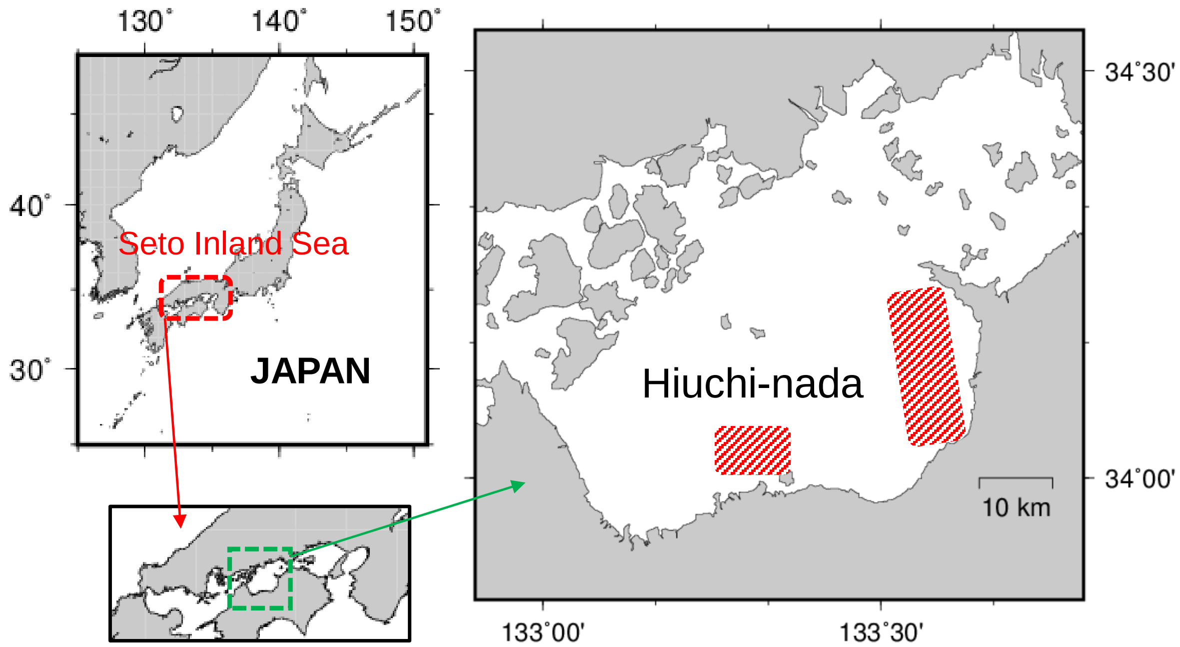
130˚
140˚
150˚
40˚
30˚
Seto Inland Sea
JAPAN
34˚30'
34˚00'
Hiuchi-nada
10 km
133˚00'
133˚30'

Fig. 2

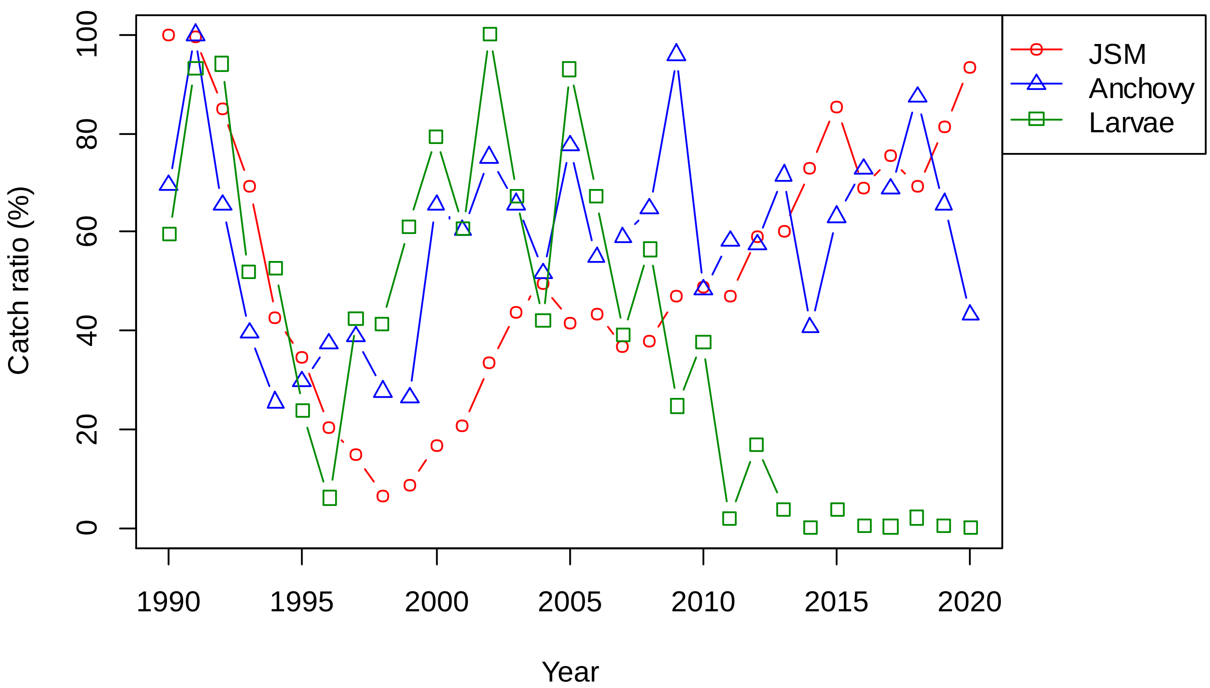
Catch ratio (%)
0
20
40
60
80
100
1990
1995
2000
2005
2010
2015
2020
Year
JSM
Anchovy
Larvae

Fig. 3

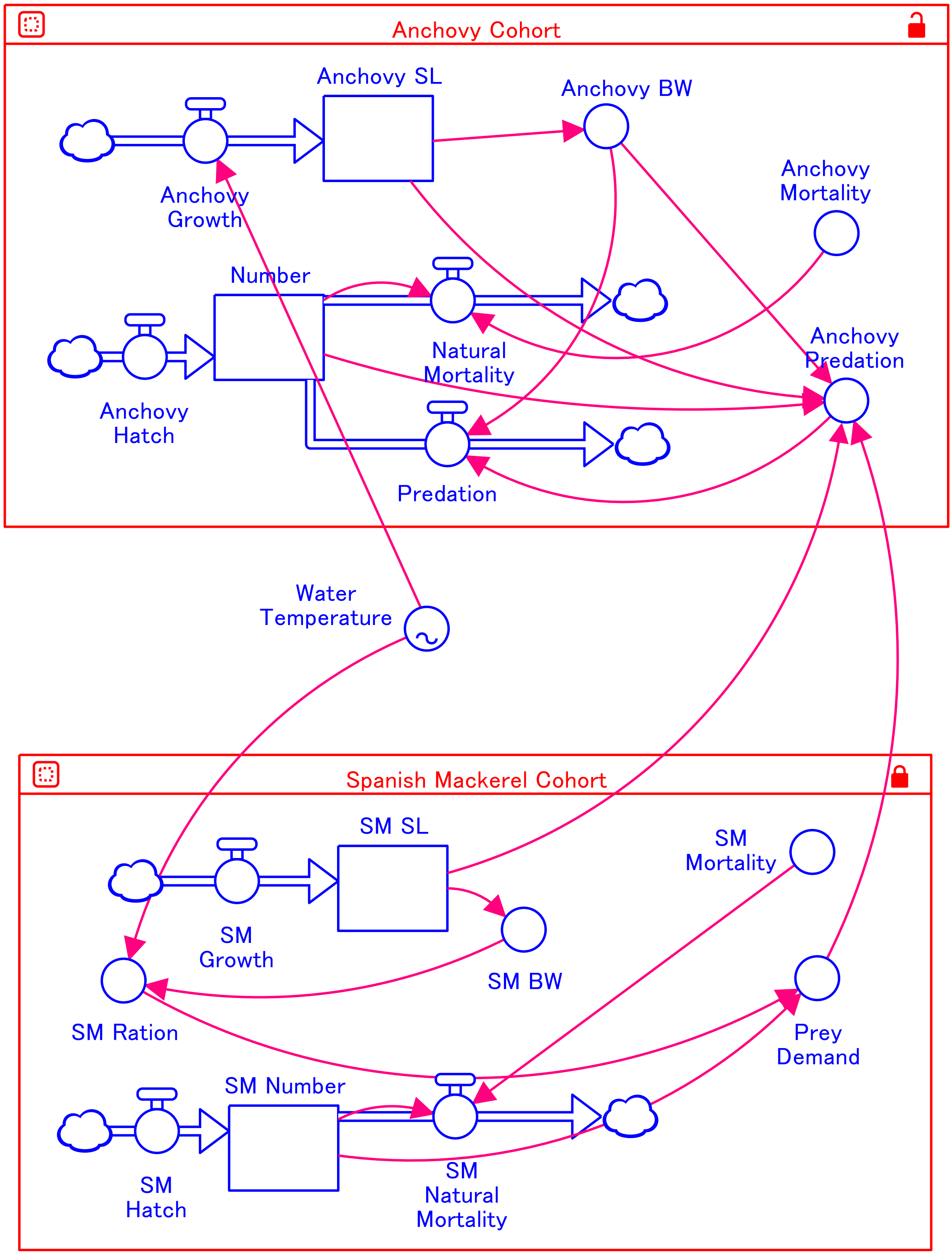

Anchovy Cohort
Anchovy SL
Anchovy BW
Anchovy Growth
Anchovy Mortality
Number
Natural Mortality
Anchovy Predation
Anchovy Hatch
Predation
Water Temperature
Spanish Mackerel Cohort
SM SL
SM Mortality
SM Growth
SM BW
SM Ration
Prey Demand
SM Number
SM Hatch
SM Natural Mortality

Fig. 4

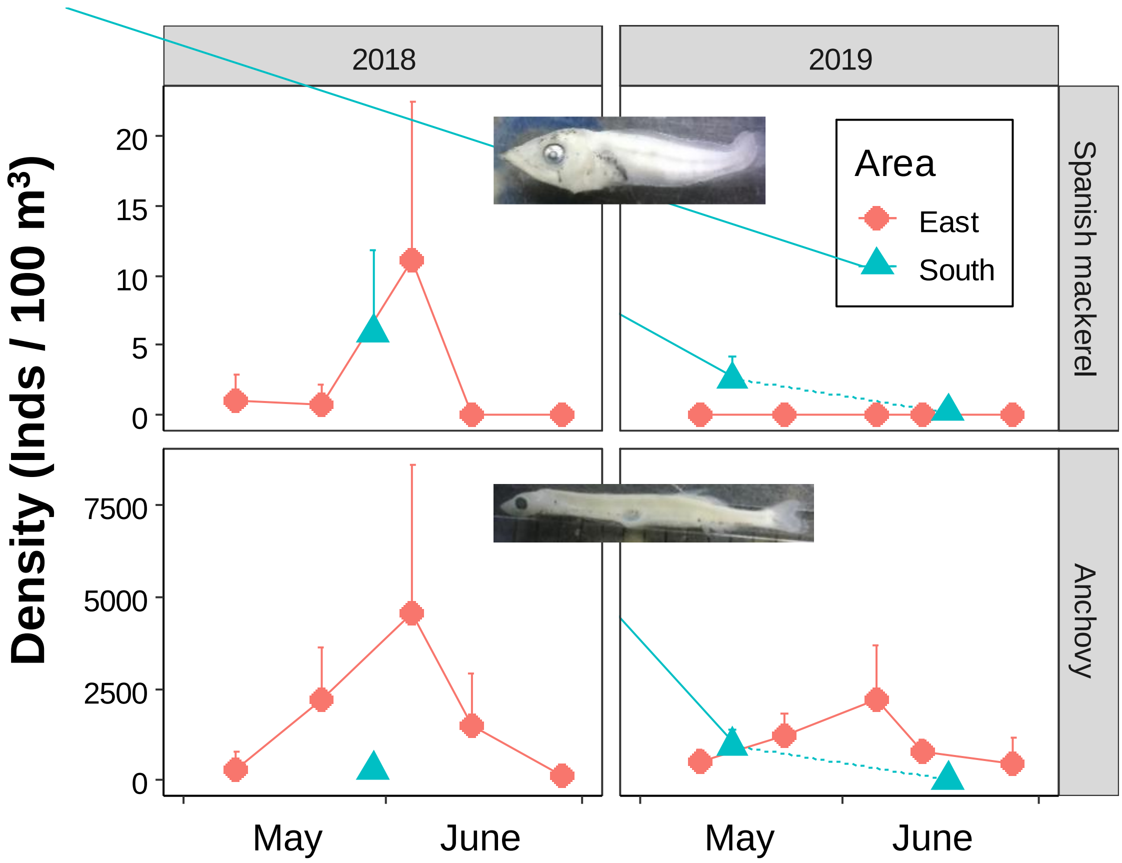
2018
2019
Density (Inds / 100 m³)
20
15
10
5
0
7500
5000
2500
0
Area
East
South
Spanish mackerel
Anchovy
May
June
May
June

Fig. 5

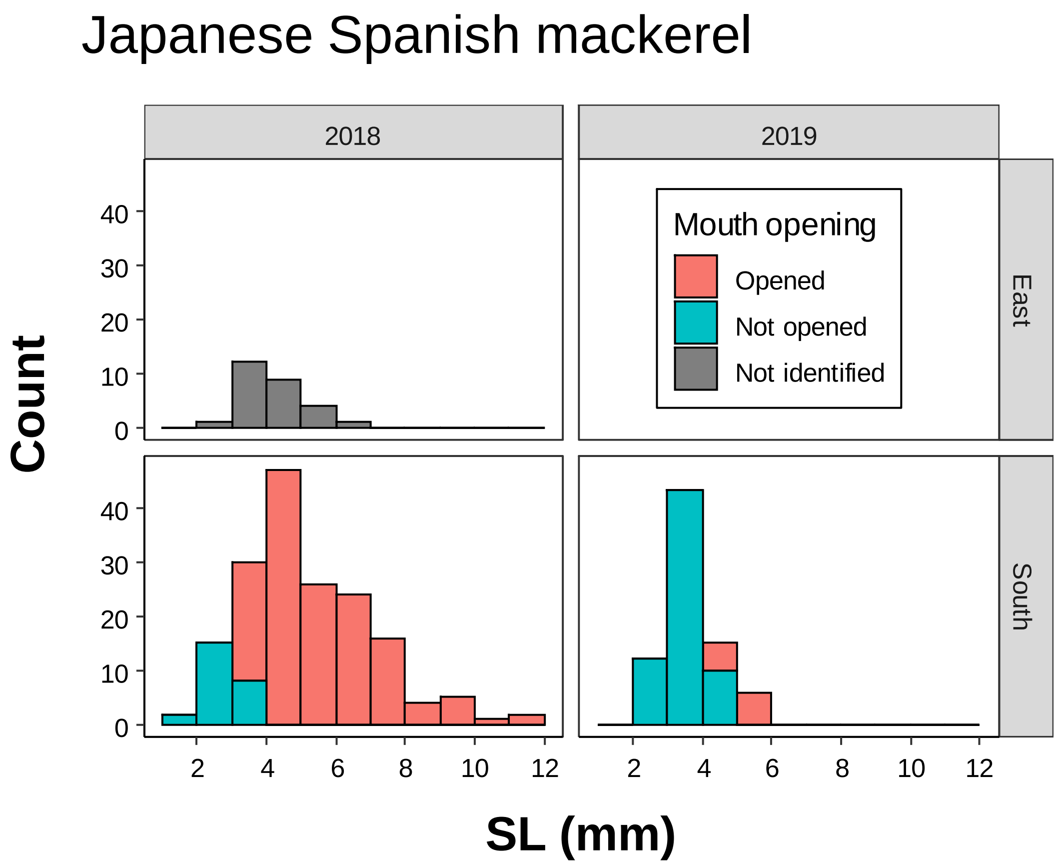
Japanese Spanish mackerel
2018
2019
Mouth opening
Opened
Not opened
Not identified
East
South
Count
SL (mm)

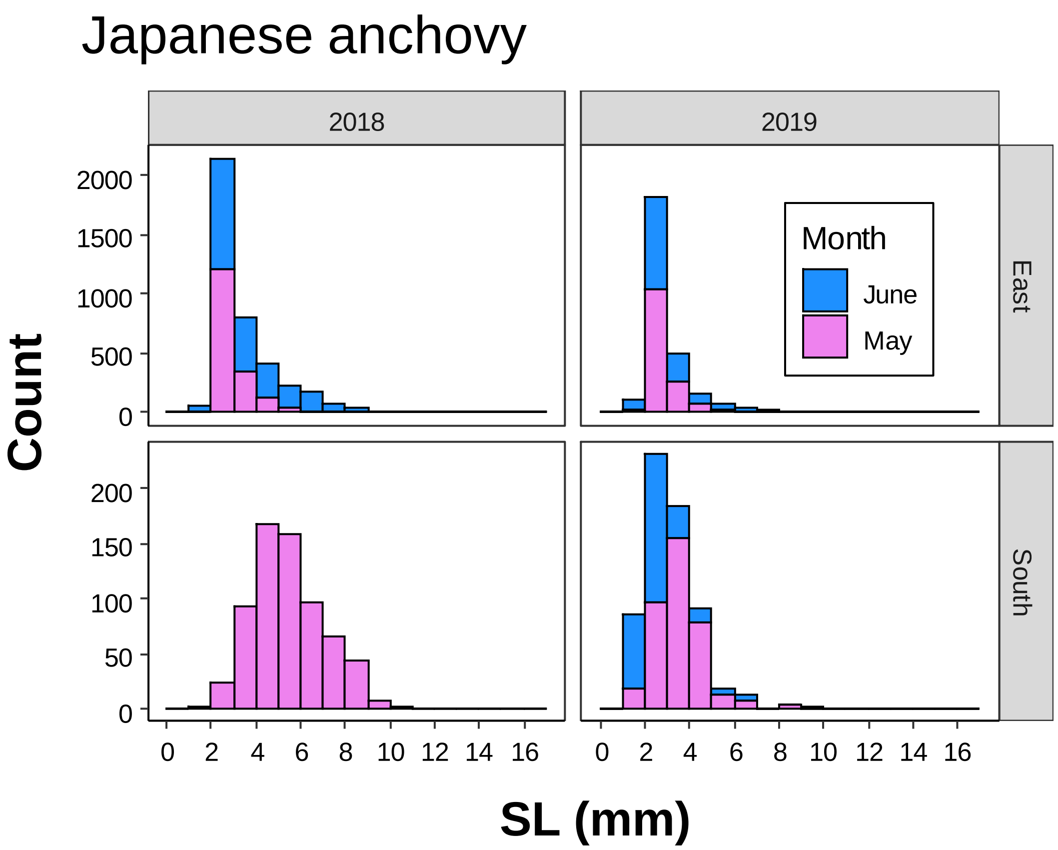
Japanese anchovy
2018
2019
Month
June
May
East
South
Count
SL (mm)

Supplementary materials can be found at:
https://doi.org/10.1016/j.dsr2.2023.105272